77-451

Unsteady Aerodynamic Modeling for Arbitrary Motions

John W. Edwards*
NASA Dryden Flight Research Center, Edwards, Calif.
and
Holt Ashley† and John V. Breakwell‡
Stanford University, Stanford, Calif.

A study is presented on the unsteady aerodynamic loads due to arbitrary motions of a thin wing and their application for the calculation of response and true stability of aeroelastic modes. The use of Laplace transform techniques and the generalized Theodorsen function for two-dimensional incompressible flow is reviewed. New applications of the same approach are shown also to yield airloads valid for quite general small motions. Numerical results are given for the two-dimensional supersonic case. Previously proposed approximate methods, starting from simple harmonic unsteady theory, are evaluated by comparison with exact results obtained by the present approach. The Laplace inversion integral is employed to separate the loads into "rational" and "nonrational" parts, of which only the former are involved in aeroelastic stability of the wing. Among other suggestions for further work, it is explained how existing aerodynamic computer programs may be adapted in a fairly straightforward fashion to deal with arbitrary transients.

Nomenclature

a_∞ = freestream speed of sound
$a, c, x_\alpha, x_\beta, r_\alpha, r_\beta, \omega_\infty, \omega_h, \beta_\beta, \mu$ = typical section parameters (definitions generally follow Ref. 2 and Sec. 9.2, Ref. 1, with $\mu = m/\pi\rho b^2$)
$A(s)$ = matrix of coefficients of transformed equations of motion
b = section semichord
$C(\bar{s})$ = $F + iG$ = generalized Theodorsen function
c_ℓ = section lift coefficient
F_p, G_p, H_1, H_2 = matrices defining Padé approximants in Eq. (57)
$H_n^{(2)}(k)$ = Hankel function of the second kind of order n
h = plunge coordinate nondimensionalized by b positive downward
$I_n(s)$ = modified Bessel function of the first kind of order n
I = identity matrix
$J_n(s)$ = Bessel function of order n
k = $\omega b/U$ = reduced frequency
$K_n(s)$ = modified Bessel function of the second kind of order n
L = lift
$\mathcal{L}[\cdot]$ = Laplace transform of $[\cdot]$
M = Mach number
M, B, K, G = inertia, damping, stiffness, and control distribution matrices
p = pressure, positive for downward loading
Q = expression defined in Eq. (7)
$Q_{\text{aero}}(s)$ = matrix of aerodynamic load coefficients
R, S_1, S_2 = vectors used to define loads, Eq. (48)
Res_ℓ = residue at the pole $s = s_\ell$
s = $\sigma + i\omega = re^{i\theta}$ = Laplace transform variable
$\bar{s}$ = sb/U
s_x = variable resulting from Laplace transformation on the x coordinate
t = time
t' = Ut/b = nondimensional time
U = freestream velocity
w_a = downwash at the airfoil
x, y, z = Cartesian coordinates
$X(s)$ = vector of transformed normal coordinates
$x(t)$ = vector of normal coordinates
x_p = vector of augmented states
x_0 = downstream extremity of wake
z_a = airfoil deflection
α = pitch coordinate, positive nose-up
β = flap deflection, positive trailing-edge down
γ_w = wake vortex strength distribution
ϵ = infinitesimal
η = $1/\pi\mu$
ξ = downstream coordinate along wake
ρ = freestream atmospheric density
τ = time
$\phi(x, y, z, t)$ = velocity potential
$\phi(\bar{s})$ = lift deficiency function
$\Phi(x, y, z, s)$ = transformed velocity potential
∇^2 = Laplacian

Superscripts

$*$ = dimensioned variable
$(\bar{\ })$ = variable nondimensionalized by b/U
T = transpose

Subscripts

a = supersonic load matrices, Eq. (25)
c = circulatory
com = command input
j = jth element of a vector
nc = noncirculatory
nr = nonrational
qs = quasisteady
r = rational
s = structural matrices, Eq. (22)

Presented as Paper 77-451 at the AIAA Dynamics Specialist Conference, San Diego, Calif., March 24-25, 1977; received March 27, 1977; revision received Sept. 21, 1978.

Index categories: Nonsteady Aerodynamics; Structural Dynamics; Aeroelasticity and Hydroelasticity.

*Aerospace Engineer. Member AIAA.
†Professor of Aeronautics, Astronautics, and Mechanical Engineering. Honorary Fellow AIAA.
‡Professor of Astronautics, Dept. of Aeronautics and Astronautics. Fellow AIAA.

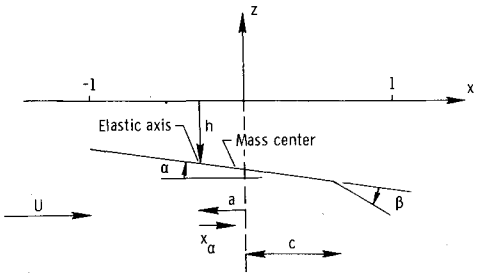

Fig. 1 Diagram of a typical section with aerodynamically unbalanced control surface.

Introduction

DURING the past decade there has been increased interest in the application of active control technology to processes which involve unsteady aerodynamics, such as active flutter control, load alleviation, fatigue reduction, and ride control. The control systems engineer requires a mathematical model of the plant to be controlled in order to design a system which will accomplish the desired objective. For these purposes, relatively simple models of unsteady aerodynamic processes have been adequate in most past design applications. The Department of Aeronautics and Astronautics, Stanford University, recently undertook a program of basic research in the active control of aeroelastic systems, with the goal of developing mathematical models and analysis techniques which will improve or simplify their design.

This paper presents the results of the unsteady aerodynamic modeling research conducted in support of this program and includes extensions thereof to cover compressible flow and three-dimensional lifting surfaces. Since modern optimal control theory provides a well developed design methodology for systems described by finite-order constant-coefficient ordinary differential equations, the goal of the modeling research has been to represent the structure and airloads in this form.

The major obstacle to be overcome is that unsteady airloads have traditionally been obtained only for simple harmonic motions. To achieve compatibility both with the structural equations of motion and with active control design techniques, airloads due to arbitrary motions are required. An implicit constraint upon this effort is the minimization or elimination of any extra state variables (augmented states) required to describe the unsteady airloads.

Unsteady Aerodynamics

General Formulation

The development of the small-disturbance partial differential equation for unsteady aerodynamic loads appears in numerous textbooks and the presentation of Bisplinghoff et al.[1] will be followed. The linearized equation satisfied by the velocity potential ϕ for unsteady, compressible flow is

$$\nabla^2\phi - \frac{1}{a_\infty^2}\frac{\partial^2\phi}{\partial t^2} - \frac{2M}{a_\infty}\frac{\partial^2\phi}{\partial x^* \partial t} - M^2\frac{\partial^2\phi}{\partial x^{*2}} = 0 \qquad (1)$$

Superposition of elementary solutions is obviously permissible. Potentials due to camber, thickness, and steady angle of attack are therefore assumed known, and the solution due to dynamic airfoil motion is sought with respect to the flat plate airfoil obtained from the projection of the actual wing onto the x-y plane.

The situation is illustrated in Fig. 1 for a three-degree-of-freedom typical section in a two-dimensional airstream. The boundary condition of tangential flow at the airfoil surface is given by

$$\frac{\partial\phi}{\partial z^*}(x^*,0,t) = w_a^*(x^*,t) = \frac{\partial z_a^*}{\partial t} + U\frac{\partial z_a^*}{\partial x^*} \qquad (2)$$

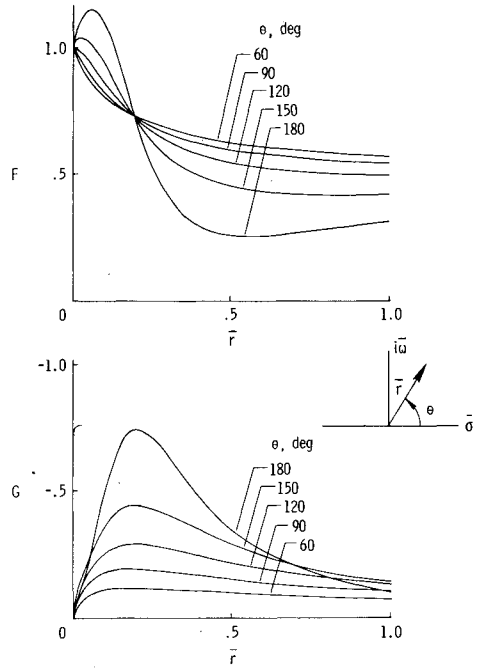

Fig. 2 Contour deformation used to evaluate inversion integral for incompressible flow.

The pressure difference acting on the airfoil, positive for downward loading, is

$$p(x^*,t) = -2\rho U\frac{\partial}{\partial x^*}\phi(x^*,0^+,t) - 2\rho\frac{\partial}{\partial t}\phi(x^*,0^+,t) \qquad (3)$$

The aerodynamic loads are obtained by appropriate integrations over the airfoil surface. For convenience, asterisks will henceforth be deleted from references to the dimensional coordinates x, y, and z.

Two-Dimensional Incompressible Flow

In this case, Eq. (1) reduces to the Laplace equation

$$\frac{\partial^2\phi}{\partial x^2} + \frac{\partial^2\phi}{\partial y^2} = 0 \qquad (4)$$

The problem is simplified because Eq. (4) is of elliptic type rather than hyperbolic when compressibility must be accounted for. References 2 and 3 give summaries of the traditional solution techniques, which have been applied to the solution of this problem. The study of unsteady airloads due to transient motions was pioneered by Wagner,[4] who calculated the lift on an airfoil at incidence, started impulsively from rest. Due to the linearity of the governing partial differential equations, it was recognized that superposition of elementary solutions could be used to calculate unsteady airloads for arbitrary motions. Garrick[5] showed that Wagner's function, $K_1(t')$, and Theodorsen's function, $C(ik)$, were a Fourier transform pair.

The application of Laplace transform techniques to unsteady aerodynamic integral equations was suggested by Jones,[6] and Sears[7] used the technique to obtain new solutions to Wagner's problem, Kussner's problem, and the oscillating airfoil problem. The discussions in Refs. 2 and 3 detail the attempts to extend Theodorsen's analysis to values of the Laplace transform variable $s=\sigma+i\omega$ off the $i\omega$ axis. The inability to rationalize this extension hinged upon the assumptions of an explicit form of airfoil motion and an infinite wake. The key to the viewpoint adopted in the present investigation is the assumption (e.g., Sears[7]) that the airfoil motion begins, not at a remote time in the past, but at $t=0$. This leads to the identification of the integrals involved as

convolution integrals and yields the transform of the circulatory lift

$$L_c(s) = -2\pi\rho bUC(\bar{s})Q(s) \tag{5}$$

Here $C(\bar{s})$ is the generalized Theodorsen function given by $K_1(\bar{s})/[K_0(\bar{s})+K_1(\bar{s})]$ with $\bar{s}=sb/U$. The modified Bessel functions in this expression are defined and analytic throughout the s plane except for branch points at the origin and infinity; and a branch cut along the negative real axis makes them single valued. Hence, by the principle of analytic continuation,[8] $C(\bar{s})$ is the unqiue operator relating $Q(s)$ to $L_c(s)$ throughout the s plane.

Except for large values of $|s|$, $K_0(\bar{s})$ and $K_1(\bar{s})$ are readily evaluated by their ascending power series expansions. The real and imaginary parts of $C(\bar{s})$ are plotted in Fig. 2 as functions of $\bar{r}$ and θ. The figure extends the calculations of Luke and Dengler[9] to $\theta=+60$ deg and $\theta=+180$ deg. The Theodorsen function is given by the curves for $\theta=90$ deg.

The time histories of unsteady loads can be calculated by the Laplace inversion integral. For plunging and pitching motions with noncirculatory terms included

$$L(s) = -\pi\rho b^3\left[s^2h(s)+\left(\frac{U}{b}s-as^2\right)\alpha(s)\right]$$

$$-2\pi\rho bUC(\bar{s})Q(s) \tag{6}$$

where

$$Q(s) = sbh(s)+U\alpha(s)+b(\tfrac{1}{2}-a)s\alpha(s)$$

The inversion integral gives

$$L(t) = \frac{1}{2\pi i}\int_{\sigma_1-i\infty}^{\sigma_1+i\infty} L(s)e^{st}ds \tag{7}$$

where σ_1 is to be chosen greater than all singularities of the integrand.

The integral of Eq. (7) may be simplified by the deformation of the contour of integration (Sears[7]) shown in Fig. 3. The portions of the contour from a to b and from c to d lie above and below the branch cut, making the integral single valued within the contour. The complex conjugate poles shown in the figure are representative of singularities which may be introduced by $Q(s)$. Since the integral is analytic at every point within the deformed contour, the integral around the contour is zero by Cauchy's integral theorem.[8] Reference 2 indicates the final reduction of Eq. (7) as

$$L(t) = L_{nc}(t)+L_r(t)+L_{nr}(t) \tag{8}$$

where

$$L_{nc} = -\pi\rho b^3[\ddot{h}+(U/b)\dot{\alpha}-a\ddot{\alpha}]$$

$$L_r = -2\pi\rho bU[\dot{h}b+U\alpha+b(\tfrac{1}{2}-a)\dot{\alpha}$$

$$-\sum_{i=1}^{n}\mathrm{Res}\phi(\bar{s})Q(s)e^{st})_{s=s_i}]$$

$$L_{nr} = -2\pi\rho bU\int_0^\infty \frac{Q(re^{i\pi})e^{-rt}}{\bar{r}[(K_0-K_1)^2+\pi^2(I_0+I_1)^2]}dr$$

where $\phi(\bar{s})=1-C(\bar{s})$. The first term, L_{nc}, is the familiar noncirculatory lift. The remaining two terms are a decomposition of the circulatory lift into portions termed "rational," L_r, and "nonrational," L_{nr}. The former is composed of the quasisteady circulatory lift and a portion due to the residues of ϕCe^{st} at all poles of $Q(s)$. The transform of this portion may be expressed as a ratio of polynomials in s,

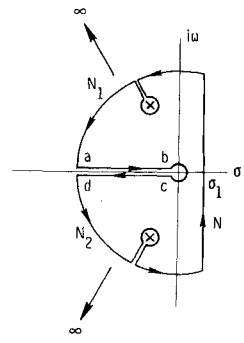

Fig. 3 The generalized Theodorsen function $C(\bar{s})=F+iG$.

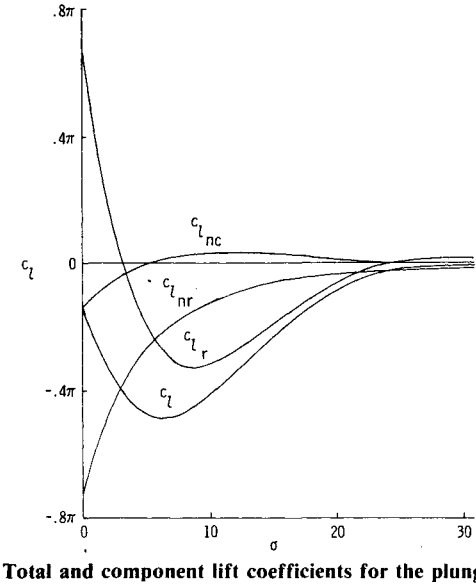

Fig. 4 Total and component lift coefficients for the plunge motion of Eq. (9).

leading to the term rational lift. The latter portion, L_{nr}, derives from the integral along the branch cut. Since its transform cannot be expressed as a ratio of polynomials in s, it is termed the nonrational lift.

Figure 4 shows the total and component lift coefficients for the plunging motion

$$L(t) = \frac{U}{b(\sigma^2+\omega^2)}[\omega-e^{-\sigma t}(\sigma\sin\omega t+\omega\cos\omega t)] \tag{9}$$

with $\sigma=\omega=0.2/\sqrt{2}$. This gives $Q(t)=Ue^{-\sigma t}\sin\omega t$ and $Q(s)=U\omega/[(s+\sigma)^2+\omega^2]$. The nonrational portion, $c_{l_{nr}}$, decays quickly for small values of t', but decays slowly for large t'. It is a monotonic function of t' and Edwards[2] shows that it approaches its final value as $1/t'^2$.

Laplace Transformation of Compressible Airloads

The calculation of unsteady airloads due to simple harmonic motion has traditionally begun with the substitution $\phi(x,y,z,t)=\phi(x,y,z)e^{i\omega t}$. This is equivalent to applying the Fourier integral transform[10] to the time variable of Eq. (1). In attempting to derive solutions with general time dependence, it is natural to apply the Laplace integral transform.[10] By defining

$$\Phi(x,y,z,s) \equiv \int_0^\infty \phi(x,y,z,t)e^{-st}dt \tag{10}$$

the three-dimensional equation of unsteady aerodynamics is transformed into

$$\Phi_{xx}+\Phi_{yy}+\Phi_{zz}-\frac{s^2}{a_\infty^2}\Phi-\frac{2Ms}{a_\infty}\Phi_x-M^2\Phi_{xx}=f(x,y,z) \tag{11}$$

where

$$f(x,y,z) = -\frac{s}{a_\infty^2}\phi(x,y,z,0)$$

$$-\frac{1}{a_\infty^2}\phi_t(x,y,z,0) - \frac{2M}{a_\infty}\phi_x(x,y,z,0) \tag{12}$$

The boundary condition is

$$\mathcal{L}[w_a(x,y,t)] = \Phi_z|_{z=0} = \left(s + U\frac{\partial}{\partial x}\right)\mathcal{L}[z_a(x,y,t)] - z_a(x,y,0) \tag{13}$$

The terms $f(x,y,z)$ in Eq. (11) and $z_a(x,y,0)$ in Eq. (13) are initial conditions resulting from the transform. Since Eq. (11) is linear, the solution can be obtained as a superposition

$$\Phi(x,y,z,s) = \Phi_1(x,y,z,s) + \Phi_2(x,y,z,s) \tag{14}$$

where Φ_2 is regarded as a known function chosen to satisfy Eq. (11) subject to the boundary condition

$$\left[\frac{\partial}{\partial z}\Phi_2\right]_{z=0} = -z_a(x,y,0) \tag{15}$$

Thus, Φ_2 takes care of the initial conditions introduced by the transformation, whereas Φ_1 satisfies a boundary value problem which is formally identical to that resulting from the assumption of simple harmonic motion with the relpacement of $i\omega$ by $s = \sigma + i\omega$:

$$\nabla^2\Phi_1 - \frac{s^2}{a_\infty^2}\Phi_1 - \frac{2Ms}{a_\infty}\frac{\partial}{\partial x}\Phi_1 - M^2\frac{\partial^2}{\partial x^2}\Phi_1 = 0 \tag{16}$$

$$\left[\frac{\partial}{\partial z}\Phi_1\right]_{z=0} = \left(s + U\frac{\partial}{\partial x}\right)\mathcal{L}[z_a] \tag{17}$$

It appears that digital programs which calculate airloads due to simple harmonic motions may be modified in a fairly straightforward manner to calculate airloads corresponding to the Φ_1 solution.

These Φ_1 solutions are linear with respect to the transformed airfoil motions, whereas those from Φ_2 are linear with respect to the initial conditions of the motion. Therefore, the corresponding generalized forces will be of the form $A_1X(s) + A_2x(0)$, where $X(s)$ and $x(0)$ are $n \times 1$ vectors of normal mode coordinates. When these are incorporated into the structural equations of motion, it is seen that only the airloads corresponding to the Φ_1 solution are required to determine stability. Hence, the flutter problem may be studied using Φ_1 alone. (The Φ_2 solution is also required if exact transient responses are desired.) The true aeroelastic modes of the system may be obtained from the equations of motion using only Φ_1. A new and exact technique is thereby provided for calculating both subcritical and supercritical behavior.

(In Ref. 11 the Laplace inversion integral was used to calculate the transient lift on an impulsively plunging airfoil in subsonic flow. Using the contour deformation of Fig. 3 and integrating along the branch cut as previously, yielded a transient lift function that did not include the characteristic subsonic starting pulse.[12] Subsequent numerical quadrature of the integral along the $i\omega$ axis using improved aerodynamic functions has successfully reproduced the indicial lift function of Ref. 12. It appears that the earlier analysis was in error in assuming that the integrals along the infinite semicircles in Fig. 3 are zero.)

It is anticipated that the decomposition indicated by Eq (14) occurs also in solutions based upon the acceleration potential ψ, since ψ and ϕ satisfy the same partial differential equation.

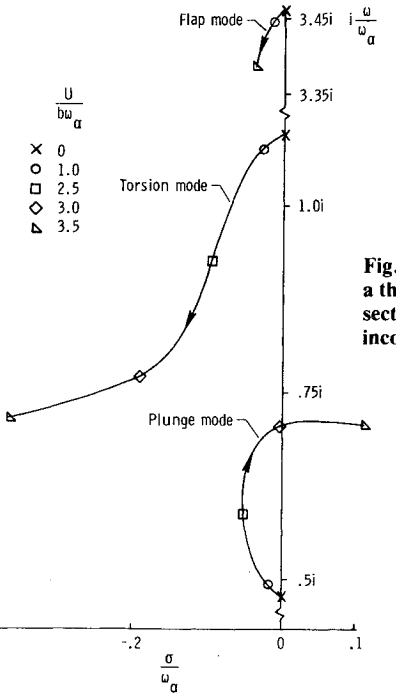

Fig. 5 Locus of roots of a three-degree-of-freedom section vs $U/b\omega_\alpha$ in incompressible flow.

Thus, programs based upon pressure doublet techniques (e.g., Ref. 13) may be modified to calculate the Laplace transforms of generalized aerodynamic loads. It must be emphasized that the resulting transform is not the total solution but corresponds to that portion which is linear in the transformed airfoil displacement modes.

Two-Dimensional Supersonic Flow

In this case, Garrick and Rubinow[14] obtained the simple harmonic loads using elementary solutions of Eq. (1) known as source-pulses and gave the forces and moments for three degrees of freedom: plunge, pitch, and trailing-edge control surface. Hassig[15] extended Garrick's treatment to cover leading-edge control surfaces. The loads due to arbitrary motions, which are linear in the transformed motion coordinates $h(s)$, $\alpha(s)$, and $\beta(s)$, may be obtained from the expressions given by Garrick by the formal replacement of k by $-i\bar{s}$. The velocity potential of Ref. 14 on the upper surface of the airfoil is transformed into

$$\Phi(x,0^+,\bar{s}) = \frac{b}{\sqrt{M^2-1}}\int_0^x w_a(\xi,\bar{s})\exp\left[-\frac{\bar{s}M^2}{M^2-1}(x-\xi)\right]$$

$$\cdot J_0\left[-i\frac{\bar{s}M}{M^2-1}(x-\xi)\right]d\xi \tag{18}$$

with the airfoil lying between $x = 0$ and $x = 1$.

Alternatively, Eq. (18) may be derived directly from Eqs. (16) and (17) following the procedure of Stewartson[16] summarized in Ref. 1 (pp. 364-367). Stewartson's Laplace transformation on x, applied to Eq. (16), leads directly to Eq. (18) with the recognition of§

$$\mathcal{L}_x^{-1}\left[\frac{1}{\sqrt{s_x^2 - a_1^2}}\right] = I_0(a_1x) \tag{19}$$

where $a_1 = \bar{s}M/(M^2-1)$. Garrick's solution in terms of J_0 is recovered by use of the relations

$$I_0(s) = J_0(se^{\frac{1}{2}\pi i}); \quad -\pi < \arg s \leq \tfrac{1}{2}\pi \tag{20a}$$

$$I_0(s) = J_0(se^{-3/2\pi i}); \quad \pi/2 < \arg s \sim \pi \tag{20b}$$

§$\mathcal{L}_x[\Phi(x,z,\bar{s})] \equiv \Phi(s_x,z,\bar{s})$.

Table 1 Three-degree-of-freedom section parameters for incompressible flow

$\omega_\alpha = 100$ rad/s	$x_\alpha = 0.2$
$\omega_h = 50$ rad/s	$r_\alpha^2 = 0.25$
$\omega_\beta = 300$ rad/s	$x_\beta = 0.0125$
$\mu = 40$	$r_\beta^2 = 0.00625$
$a = -0.4$	
$c = 0.6$	

Table 2 Three-degree-of-freedom typical section parameters for supersonic flow

$\omega_\alpha = 100$ rad/s	$x_\alpha = 0.2$
$\omega_h = 50$ rad/s	$r_\alpha^2 = 0.25$
$\omega_\beta = 317$ rad/s	$x_\beta = 0.0125$
$\mu = 40$	$r_\beta^2 = 0.00625$
$a = 0$	$b = 1.35$ m
$c = 0.6$	$a_\infty = 333$ m/s

with recognition that the Bessel function J_0 is single valued. The foregoing inverse transform leads to $J_0\{-[i\bar{s}M/(M^2-1)]x\}$, verifying Eq. (18) as the generalized velocity potential for supersonic two-dimensional flow.

Edwards[2] gives the generalized loads resulting from Eq. (18). These loads do not involve a single nonrational transform, such as $C(\bar{s})$ for the $M=0$ case, but contain a number of nonrational functions. The exact transient time responses of the loads due to indicial motions have been determined by Chang[17] and Lomax et al.[12] These responses are typified by discontinuous first derivatives and different functional dependence in various time zones. These facts suggest that the calculation of general transients using inverse Laplace transformation could be laborious. The primary use of these transformed loads is for the investigation of airfoil stability, i.e., the flutter problem. Examples of calculations using these generalized supersonic loads are given in the following sections.

Solution of the Aeroelastic Equations of Motion

The transformed equations of motion of the section shown in Fig. 1 may be written as

$$\mathfrak{A}(s)X(s) = G\beta_{\text{com}}(s) \tag{21}$$

where

$$\mathfrak{A}(s) = M_s s^2 + K_s - Q_{\text{aero}}(s) \tag{22}$$

$$X^T(s) = [h(s)\alpha(s)\beta(s)] \tag{23}$$

$Q_{\text{aero}}(s)$ is the matrix of aerodynamic coefficients. In incompressible flow

$$Q_{\text{aero}}(s) = \frac{1}{\pi\mu}\left(\frac{U}{b}\right)^2 \{M_{nc}\bar{s}^2 + B_{nc}\bar{s} + K_{nc} + C(\bar{s})R[S_2\bar{s} + S_1]\} \tag{24}$$

The matrices in Eqs. (21-24) are defined in the Appendix. In supersonic flow

$$Q_{\text{aero}}(s) = \frac{8\rho b^2 U^2 \bar{s}^2}{\sqrt{M^2-1}}\{M_a(\bar{s})\bar{s}^2 + B_a(\bar{s})\bar{s} + K_a(\bar{s})\} \tag{25}$$

These supersonic load matrices are given in Ref. 2.

Root Loci of Aeroelastic Modes

Equation (21) is linear, and the stability of the airfoil section is determined, therefore by the homogeneous reduction

$$\mathfrak{A}(s)X(s) = 0 \tag{26}$$

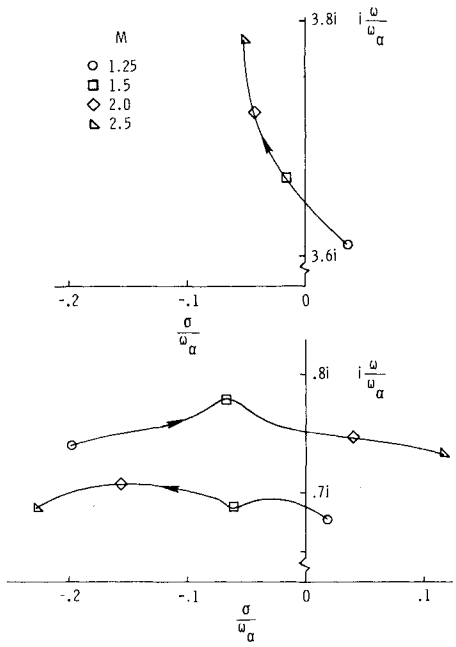

Fig. 6 Locus of roots of a three-degree-of-freedom section vs $U/b\omega_\alpha$ in supersonic flow.

The loads, Eqs. (24) or (25), are valid for arbitrary values of the Laplace transform variable s. Hence, they may be combined with the equations of motion and the stability of the system determined by examining the zeroes of the determinant of $\mathfrak{A}(s)$. Similar calculations are mentioned by Dengler et al.[18] in attempting to defend their generalized Theodorsen function but have evidently never been published.

Since the loads are not rational functions of $\bar{s}$, a computer program was developed to determine numerically the roots of the characteristic equation by iteration. For the systems analyzed here it was feasible to expand the determinant numerically. A gradient search algorithm was employed to locate its zeroes, which are the poles of the aeroelastic system. The gradient was calculated by finite differences in the s plane, and the performance of the algorithm was quite satisfactory for the systems treated; those went up to four degrees of freedom (eighth order).

Incompressible, Two-Dimensional Flow

Table 1 lists the structural and geometrical parameters required for the three-degree-of-freedom system used in the following calculations. The frequency ratio $\omega_h/\omega_\alpha = 0.5$, and the natural frequency of the flap mode is three times that of the torsion mode.

The loads contain the generalized Theodorsen function $C(\bar{s})$, which depends on s and U/b. Thus, with U/b specified, the roots of the equations of motion may be determined by iteration in the s plane. Figure 5 shows the exact locus of roots of the three-degree-of-freedom system of Table 1 as a function of $U/b\omega_\alpha$. The inertia coupling of the three modes causes the still-air natural frequencies to be shifted from their uncoupled values. As the airspeed increases, the bending and torsion modes are seen to approach each other in the stable left-hand plane, with the bending branch becoming the flutter mode at $U/b\omega_\alpha \approx 3.0$.

The circular disk $|s| < 1000$ rad/s was searched for other isolated singularities and none were found at the airspeeds indicated in Fig. 2. Edwards[2] demonstrates that at higher airspeeds an additional pole does appear on the positive real axis. This pole occurs in addition to the six "structural" poles and is identified as an aperiodic divergence mode which originates at the origin at the static divergence speed.

The root locus format is used for the presentation of results rather than the conventional $U-g$, $U-\omega$ plots (cf. Ref. 1,

Chap. 9) since the ability to calculate generalized aerodynamics makes this a more natural format. It avoids the numerical problems of root sorting, because the loci do not cross each other. It is required for active control design applications.

Supersonic, Two-Dimensional Flow

Table 2 lists the parameters of the three-degree-of-freedom section used to illustrate the aeroelastic root loci in supersonic flow. The loads, Eq. (25), are functions of the generalized supersonic reduced frequency parameter, $\bar{\omega} = -i[2\bar{s}M^2/(M^2-1)]$, and the algorithm described earlier may again be used for the determination of the system poles.

The loci of roots of this section are shown in Fig. 6 as a function of Mach number. At $M=1.25$, both the lowest frequency, coupled-bending-torsion mode and the flap mode are unstable. It is believed that the flap mode is primarily a "single-degree-of-freedom" flutter. As the Mach number increases, both of these modes become stable at $M\cong 1.4$. Above $M\cong 1.8$ the remaining coupled-bending-torsion mode flutters. Hence, for the mass ratio $\mu=40$, the range of linear stability for this section is $1.4\leq M\leq 1.8$.

The aerodynamic matrices M_a, B_a, and K_a are derived from terms composed of finite integrals of exponentially weighted Bessel functions of integer order, as shown by Eq. (18). Since the ordinary Bessel functions, $J_i(s)$, are single-valued analytic functions of s, there will be no branch points of the characteristic equation as in the incompressible case. However, a review of supersonic indicial aerodynamics (e.g., Lomax et al.[12]) leads to the suspicion that the supersonic characteristic equation must have more singularities than the six structural poles, because these six poles cannot yield the complex indicial functions. Since the poles of the system are the zeroes of the determinant of the matrix of coefficients, a search was made for additional zeroes, of this function. Because the terms involved in the aerodynamic matrices do not become infinite in the finite s plane, the determinant has no poles and examination of the number of 360-deg phase changes of the determinant around a closed contour will directly indicate the number of zeroes within the contour (Ref. 8, p. 61). A circular contour of radius 1000 rad/s centered at the origin yielded six 360-deg phase changes of the determinant, accounting for only the six known structural poles. Further searching located the first additional zero as a complex conjugate pair at $s=-1315.\pm i1501$, over 20 times the frequency of the flutter mode. However, it is anticipated that an infinite sequence of additional zeroes of increasing modulus does exist, due to the oscillatory nature of the exponential weighting factor in the integrand of Eq. (18), and accurate transient response calculations would require the evaluation of a number of these zeros of lowest modulus and their corresponding residues. Fortunately, the flutter problem can be studied by determining only the zeros due to the structural poles.

Inversion Integral for Arbitrary Airfoil Motions

Returning to the case of incompressible flow, it is possible to calculate exact transient motions from Eq. (21) using the Laplace inversion integral. If $\mathrm{Det}[\mathfrak{A}(s)]\neq 0$, $[\mathfrak{A}(s)]^{-1}$ exists and the solution of Eq. (21) is

$$X(s)=[\mathfrak{A}(s)]^{-1}G\beta_{\mathrm{com}}(s) \tag{27}$$

The transform of the jth mode is

$$X_j(s)=\frac{N_j(s)}{D(s)}\beta_{\mathrm{com}}(s) \tag{28}$$

and

$$x_j(t)=\frac{1}{2\pi i}\int_{\sigma_1-i\infty}^{\sigma_1+i\infty}\frac{N_j(s)}{D(s)}\beta_{\mathrm{com}}(s)e^{st}\mathrm{d}s \tag{29}$$

Cramer's rule is used to evaluate $X_j(s)$, with $D(s)=\mathrm{Det}[\mathfrak{A}(s)]$ and $N_j(s)=\mathrm{Det}[\mathfrak{A}(s)]$ with the jth column of $\mathfrak{A}(s)$ replaced by G. Due to the complexity of Eq. (27) it is no longer feasible to obtain analytic expressions for the integrand, but it may be evaluated numerically. Since the elements of $\mathfrak{A}(s)$ contain $C(\bar{s})$, $X_j(s)$ will have a branch cut along the negative real axis and the contour of integration may be deformed as shown in Fig. 4, giving

$$x_j(t)=\sum_{\ell=1}^{N}\mathrm{Res}_\ell e^{s_\ell t}-\frac{1}{2\pi i}\int_0^\infty\left[x_j(re^{i\pi})-x_j(re^{-i\pi})\right]e^{-rt}\mathrm{d}r \tag{30}$$

where s_ℓ; $\ell=1,2,\ldots,N$ are the poles of Eq. (28) and the residues are evaluated at the poles by

$$\mathrm{Res}_\ell=\frac{N_j(s_\ell)}{D'(s_\ell)}\cong\frac{N_j(s_\ell)}{D(s)-D(s_\ell)}(s-s_\ell)\cong\frac{N_j(s_\ell)}{D(s)}\Delta s \tag{31}$$

with $\Delta s=s-s_\ell$. [Since the poles are determined numerically by iteration, $D(s_\ell)\cong 0$].

The poles due to the structural equations of motion may be assumed to be complex conjugates with $s_\ell=a_\ell-ib_\ell$, $s_{\ell+1}=a_\ell-ib_\ell$. Poles due to $\beta_{\mathrm{com}}(s)$ may be real or complex, but for the following development it is assumed there are N complex poles within the contour. Since $x_j(t)$ must be real, the integrand must be pure imaginary and therefore $X_j(re^{i\pi})$ and $X_j(re^{-i\pi})$ are complex conjugate expressions. With $N_j(s_\ell)=N_{j\ell}^R+iN_{j\ell}^I$, Eq. (30) becomes

$$x_j(t)=\sum_{\ell=1}^{N/2}2e^{a_\ell t}[N_{j\ell}^R\cos b_\ell t-N_{j\ell}^I\sin b_\ell t]$$

$$-\frac{1}{\pi}\int_0^\infty Im[X_j(re^{i\pi})]e^{-rt}\mathrm{d}r \tag{32}$$

or

$$x_j(t)=x_{j_r}(t)+x_{j_{nr}}(t) \tag{33}$$

The incompressible flow transient response of the three-degree-of-freedom section of Table 1 has been calculated for a unit step input torque command to the flap, $\beta_{\mathrm{com}}(s)=1/s$, for $U/b\omega_\alpha=2.9$. Figure 2 indicates that the bending mode has a subcritical damping ratio of $\zeta=0.03$ at this airspeed. To study the effect of changes in airspeed on the nonrational portion of the response, $Im[h(re^{i\pi})]$ and $Im[\alpha(re^{i\pi})]$ are plotted in Fig. 7 for $U/b\omega_\alpha=2.0$, 2.9, and 3.5. At time t, $x_{j_{nr}}(t)$ is given by the integral of the product of the function shown in the figure and e^{-rt}. Hence, the value of $x_{j_{nr}}(0)$ is proportional to the area under the curves; since all of the functions go to zero at $r=0$, $\lim_{t\to\infty}x_{j_{nr}}(t)=0$. In other words, the nonrational portion of the response does not participate in the motion characteristic of an unstable fluttering airfoil. Note that all of the curves shown in Fig. 5 are smoothly varying functions of r and $U/b\omega_\alpha$, even as the airfoil flutters at $U/b\omega_\alpha\cong 3.0$.

The poles and residues required to calculate Eq. (32) were evaluated and the integral was solved by quadrature. The component and total transient responses of the plunge and torsion modes are shown in Fig. 8. In this case, the contour integral about the infinitesimal circle at the origin in Fig. 3 will be nonzero, its value being the steady-state $x_j(t)$ due to the step change in β_{com}. These steady-state limiting amplitudes were determined from Eq. (21) by applying the final-value theorem, $\lim_{s\to 0}sX_j(s)=\lim_{t\to\infty}x_j(t)$, rather than by contour integration. The oscillatory harmonic mode superimposed on $\alpha_r(t)$ [and, to a smaller extent, on $h_r(t)$] is due to a very lightly damped flap mode which is not shown. The nonrational portion of $h(t)$ is 75% of the rational portion of $h(t)$ at $t=0$, whereas the corresponding percentage for $\alpha(t)$ in only 15%. As in the case of the transient loads, the

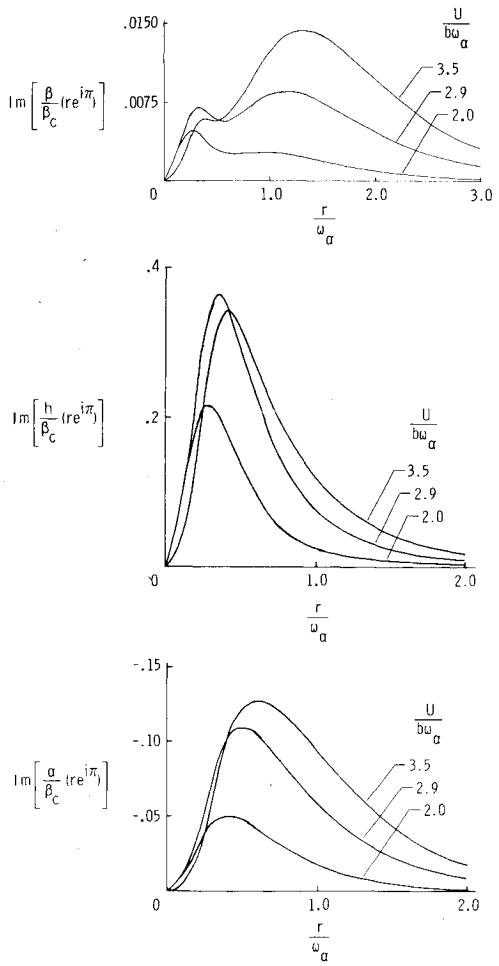

Fig. 7 Integrands of nonrational portion of response due to step command to the flap, $M=0$.

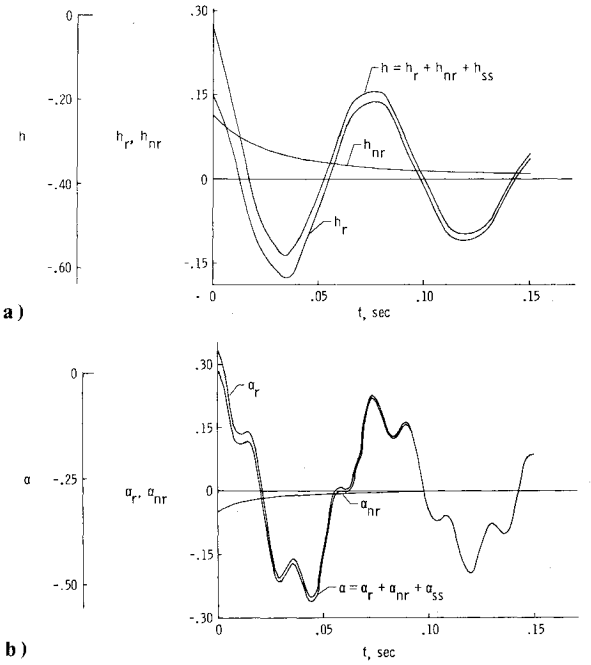

Fig. 8 Rational, nonrational, and total response due to a step command to the flap, $M=0$: a) plunge response, b) pitch response.

nonrational portion of the response is characterized by a rapid initial decay followed by a slow asymptotic decay, the entire function decreasing monotonically with t. Since the response of a mechanical system to a step input in torque must start at zero, the sum of the rational and nonrational portions should cancel the steady-state value of $x_j(t)$. Hence, the small nonzero value of $\alpha(0)$ and the larger value of $h(0)$ are attributed to numerical inaccuracies in evaluating the residues.

The following comments are made with respect to Fig. 8.

1) The oscillatory motions typifying flutter phenomena are due entirely to the rational portion of the response. If a method were available for modeling only this portion of the system it would serve to describe the pertinent features of the flutter problem.

2) The effect of the nonrational portion on the oscillatory total response would tend to complicate the determination of the damping ratio of the rational portion. Techniques for determining damping ratios which do not address this fact may produce inconsistent estimates. This effect may be aggravated in cases with random structural excitations. If an estimate of the nonrational response is available, subtraction of this estimate from the total response is likely to improve the damping estimates.

Padé Approximations and Augmented State Methods

In this section an approximate technique of representing unsteady aerodynamic loads will be evaluated. The particular scheme for obtaining load expressions for arbitrary values of s is the approximation of the simple harmonic loads, tabulated for several values of k, by a rational function of s. This approximation may be designed to produce a best fit in a least-squares sense of the tabulated loads. The rational function describing the load(s) is then incorporated into the model of the system as additional ordinary differential equations, whose transforms correspond to the approximating function. These augmented states increase the order of the system and allow the convenience of linear eigenvalue techniques in the ensuing analysis. Hassig[19] is representative of several authors who have employed various versions of this approach for both two- and three-dimensional applications.

Incompressible Two-Dimensional Flow

Augmented state methods for this flow regime derive from Jones'[20] exponential approximation of Wagner's indicial loading function. Laplace transformation of this formula yields the following approximation to $C(\bar{s})$

$$C(\bar{s}) \cong \frac{0.5\bar{s}^2 + 0.2808\bar{s} + 0.01365}{\bar{s}^2 + 0.3455\bar{s} + 0.01365} \tag{34}$$

This rational transform may be evaluated at $\bar{s} = \bar{r}e^{i\theta}$. Comparisons of the resulting values with corresponding values computed from the generalized Theodorsen function indicate that Eq. (34) is a good representation of $C(\bar{s})$ for values of s near the $i\omega$ axis. The agreement deteriorates as θ increases beyond 90 deg due to the proximity of the isolated poles of Eq. (34) at $\bar{s} = -0.0455$ and -0.3.

A unique feature of the incompressible case is that all of the circulatory loads involve the single nonrational function, $C(\bar{s})$, greatly simplifying the approximation problem. The differential equations representing the approximation of Eq. (34) are incorporated into the section equations of motion using two augmented states $x_p^T = [x_1 x_2]$ as

$$\begin{bmatrix} I & 0 & 0 \\ 0 & M' & 0 \\ 0 & 0 & I \end{bmatrix} \begin{bmatrix} \dot{x} \\ \ddot{x} \\ \dot{x}_p \end{bmatrix} = \begin{bmatrix} 0 & I & 0 \\ -K' & -B' & D \\ E_1 & E_2 & F_p \end{bmatrix} \begin{bmatrix} x \\ \dot{x} \\ x_p \end{bmatrix} + \begin{bmatrix} 0 \\ G \\ 0 \end{bmatrix} \beta_{\text{com}} \tag{35}$$

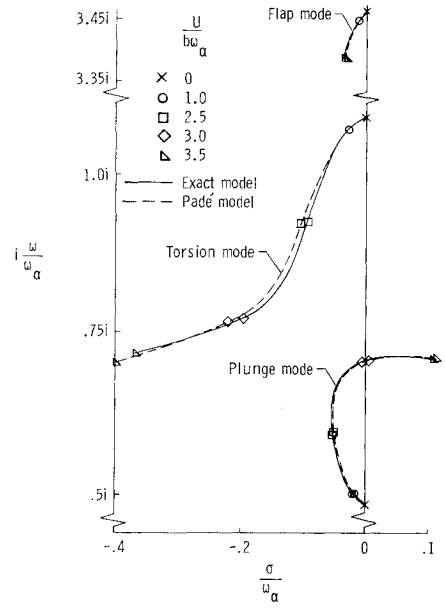

Fig. 9 Comparison of roots obtained using the generalized Theodorsen function and Jones' approximation to $C(s)$ as a function of $U/b\omega_\alpha$.

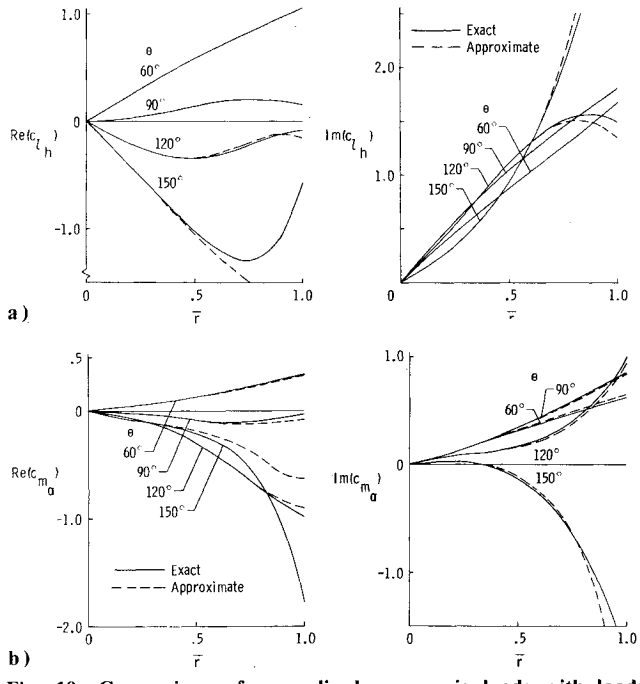

Fig. 10 Comparison of generalized supersonic loads with loads computed from matrix Padé approximants as functions of $\bar{r}$ and θ at $M=2.0$: a) c_{l_h}, b) c_{m_α}.

where

$$M' = M_s - \eta M_{nc}$$

$$K' = K_s - \eta (U/b)^2 (K_{nc} + 0.5RS_1)$$

$$B' = B_s - \eta (U/b)(B_{nc} + 0.5RS_2)$$

$$D = \eta (U/b) R[0.006825(U/b)^2 0.10805(U/b)]$$

$$F_p = \begin{bmatrix} 0 & I \\ -0.01365(U/b)^2 & -0.3455(U/b) \end{bmatrix}$$

$$E_1 = (U/b)\begin{bmatrix} 0 \\ \hline S_1 \end{bmatrix}, \quad E_2 = \begin{bmatrix} 0 \\ \hline S_2 \end{bmatrix}$$

$$\eta = l/\pi\mu, \qquad x^T = [h \quad \alpha \quad \beta]$$

The matrices in Eq. (35) are functions of (U/b), and the eigenvalues of the equation are approximate roots of the aeroelastic equations of motion. Figure 9 compares these eigenvalues to the exact root from Fig. 5. From the close agreement shown, it may be concluded that the linear, rational model of the incompressible two-dimensional section, Eq. (35), is interchangeable with the exact model, Eq. (21), for the purposes of engineering design.

The Matrix Padé Approximate Technique

The approximation technique of the last section involves two steps. First, an exponential approximation of an indicial load function must be obtained, and then a rational transfer function is obtained by Laplace transformation of this expression. The essential step is the latter, and techniques have been developed for obtaining these Padé approximants directly from readily calculated simple harmonic loads. A Padé approximant[21] of an analytic function of s is a ratio of two polynomials in s (rational function) which approximates the original function. When the latter is known only in tabulated form, as is the case for unsteady airloads, Padé approximants are constructed by fitting an assumed function to the tabulated data. The order of the Padé approximant is the highest power of s in the denominator polynomial. As this order increases, the fit of the original function will become better. However, this increased accuracy is offset by the higher-order models which must be manipulated. Roger and Hodges[22] describe the design of the B-52 flutter mode control system, in which each load was approximated by a separate Padé approximant. The resulting model contained well over 100 augmented states.

In order to reduce the number of augmented states, Vepa[23,24] introduced matrix Padé approximants. The philosophy underlying this improvement is that the individual loads may be approximated by suitable linear combinations of shared eigenvalues. Edwards[2] gives the following state-space representation of Vepa's matrix Padé approximants:

$$\left.\begin{aligned} \dot{x}_p &= F_p x_p + G_p x \\ \frac{L}{\rho b^2 U^2} &= x_p + H_1 x + H_2 \dot{x} \end{aligned}\right\} \tag{36}$$

These equations may be added to the section equations of motion giving the following augmented state model

$$\begin{bmatrix} I & 0 & 0 \\ 0 & M_s & 0 \\ 0 & 0 & I \end{bmatrix} \begin{bmatrix} \dot{x} \\ \ddot{x} \\ \dot{x}_p \end{bmatrix} = \begin{bmatrix} 0 & I & 0 \\ (-K_s + \eta' H_1) & (-B_s + \eta' H_2) & I\eta' \\ G_p & 0 & F_p \end{bmatrix} \begin{bmatrix} x \\ \dot{x} \\ x_p \end{bmatrix} + \begin{bmatrix} 0 \\ G \\ 0 \end{bmatrix} \beta_{\text{com}} \tag{37}$$

For structural equtions of motion with n degrees of freedom, Eq. (37) describes a model containing only n augmented states. This is a significant reduction in the order of the final system model.

Using Vepa's technique, Edwards constructed matrix Padé approximants of two-dimensional supersonic loads at $M=1.5$, 2.0, and 2.5. These approximate loads may be evaluated for $\bar{s}=\bar{r}e^{i\theta}$, and Fig. 10 compares these values at $M=2.0$ with those obtained from the generalized supersonic load expression for lift coefficient due to plunging, c_{l_h}, and

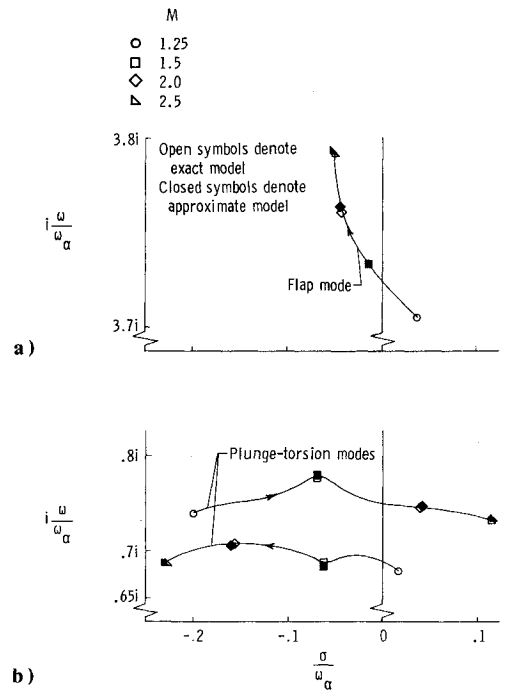

Fig. 11 Comparison of roots obtained using generalized supersonic loads and matrix Padé approximants as a function of M. Open symbols denote exact model; closed symbols denote approximate model.

pitching moment coefficient due to pitching, c_{m_α}. For $\bar{r}<0.5$ the approximate loads are in excellent agreement with the exact loads.

The eigenvalues of Eq. (37) are estimates of the exact roots of the aeroelastic system. Figure 11 compares these eigenvalues at $M=1.5$, 2.0, and 2.5 with the exact results from Fig. 5. The agreement is excellent.

The matrix Padé approximate technique is thus a viable method of predicting the stability of aeroelastic systems. However, for the purposes of active control of such systems, the large number of augmented states are not desirable. References 2 and 11 describe a technique by which the rational portion of aeroelastic systems may be modeled with no augmented states.

Conclusions

Repeating the analysis due to Sears,[7] the generalized Theodorsen function relating arbitrary airfoil motions to unsteady airloads in incompressible flow has been derived in the Appendix, using Laplace transform techniques. Inverse Laplace transformation of the resulting expressions gives exact transient responses of unsteady airfoils and airfoil motions. The airfoil response is characterized by a portion due to a rational transform and a portion due to a nonrational transform. The nonrational portion does not participate in the oscillatory response characteristic of fluttering airfoils. The same transformation technique applied to the case of compressible flow results in the derivation of generalized airload expression for two-dimensional supersonic flow, as well as a procedure whereby similar three-dimensional generalized forces can be calculated from existing computer programs.

Root loci are also calculated for the true aeroelastic modes of the two-dimensional airfoil in incompressible and supersonic flow. Finally, approximation techniques involving augmented states are evaluated and shown to give good agreement with exact calculations for values of complex reduced frequency near the imaginary axis.

Appendix: Definitions of Matrices Appearing in Eqs. (21-24)

$$M_s=\begin{bmatrix} 1 & x_\alpha & x_\beta \\ x_\alpha & r_\alpha^2 & [r_\beta^2+x_\beta(c-a)] \\ x_\beta & [r_\beta^2+x_\beta(c-a)] & r_\beta^2 \end{bmatrix}$$

$$K_s=\begin{bmatrix} \omega_h^2 & 0 & 0 \\ 0 & r_\alpha^2\omega_\alpha^2 & 0 \\ 0 & 0 & r_\beta^2\omega_\beta^2 \end{bmatrix}$$

$$G=\begin{bmatrix} 0 \\ 0 \\ r_\beta^2\omega_\beta^2 \end{bmatrix}$$

$$M_{nc}=\begin{bmatrix} -\pi & \pi a & T_1 \\ \pi a & -\pi(1/8+a^2) & -2T_{13} \\ T_1 & -2T_{13} & (1/\pi)T_3 \end{bmatrix}$$

$$B_{nc}=\begin{bmatrix} 0 & -\pi & T_4 \\ 0 & \pi(a-\tfrac{1}{2}) & -T_{16} \\ 0 & -T_{17} & (-1/\pi)T_{19} \end{bmatrix}$$

$$K_{nc}=\begin{bmatrix} 0 & 0 & 0 \\ 0 & 0 & -T_{15} \\ 0 & 0 & (-1/\pi)T_{18} \end{bmatrix}$$

$$R^T=[-2\pi \quad 2\pi(a+\tfrac{1}{2}) \quad -T_{12}]$$

$$S_1=[0 \quad 1 \quad (1/\pi)T_{10}]$$

$$S_2=[1 \quad (\tfrac{1}{2}-a) \quad (1/2\pi)T_{11}]$$

The constants T_i are defined in Ref. 25.

Acknowledgment

This research constitutes a portion of the first author's doctoral dissertation. Grateful acknowledgment is made of the National Space Club's Dryden Fellowship which supported the first parts of this research, which was also supported under NASA contract No. NSG-4002 and Air Force Contract AFOSR 74-2712.

References

[1] Bisplinghoff, R. L., Ashley, H., and Halfman, R. L., *Aeroelasticity*, Addision-Wesley, Reading, Mass., 1955.

[2] Edwards, J. W., "Unsteady Aerodynamic Modeling and Active Aeroelastic Control," Doctoral Disseration, Dept. of Aeronautics and Astronautics, Stanford University, Stanford, Calif., to be published.

[3] Edwards, J. W., "Unsteady Aerodynamic Modeling for Arbitrary Motions," *AIAA Journal*, Vol. 15, April 1977, pp. 593-595.

[4] Wagner, H., "Uber die Entstehung des dynamischen Auftriebs von Tragflugeln," *Zeitschrift für angewandte Mathematik and Mechanik*, Bd. 5, Heft 1, Feb. 1925, pp. 17-35.

[5] Garrick, I. E., "On Some Reciprocal Relations in the Theory of Nonstationary Flows," NACA Rept. 629, 1938.

[6] Jones, R. T., "Operational Treatment of the Nonuniform Lift Theory to Airplane Dynamics," NACA TN 667, 1938.

[7] Sears, W. R., "Operational Methods in the Theory of Airfoils in Non-Uniform Motion," *Journal of the Franklin Institute*, Vol. 230, July 1940, pp. 95-111.

[8]Carrier, G. F., Krook, M., and Pearson, C. E., *Functions of a Complex Variable*, McGraw-Hill Book Co., New York, 1966.

[9]Luke, Y. and Dengler, M. A., "Tables of the Theodorsen Circulation Function for Generalized Motion," *Journal of Aeronautical Sciences*, July 1951, pp. 478-483.

[10]Tranter, C. J., *Integral Transforms in Mathematical Physics*, Chapman and Hall Ltd., London, 1971.

[11]Edwards, J. W., Breakwell, J. V., and Bryson, A. E., Jr., "Active Flutter Control Using Generalized Unsteady Aerodynamic Theory," *Journal of Guidance and Control*, Vol. 1, Jan.-Feb. 1978, pp. 32-40.

[12]Lomax, H., Heaslet, M. A., Fuller, F. B., and Sluder, L., "Two-and-Three-Dimensional Unsteady Lift Problems in High-Speed Flight," NACA Rept. 1077, 1952.

[13]Watkins, C. E., Woolston, D. S., and Cunningham, H. J., "A Systematic Kernel Function Procedure for Determining Aerodynamic Forces on Oscillating or Steady Finite Wings at Subsonic Speeds," NASA TR-48, 1959.

[14]Garrick, I. E. and Rubinow, S. I., "Flutter and Oscillating Airforce Calculations for an Airfoil in Two Dimensional Supersonic Flow," NACA Rept. No. 846, 1946.

[15]Hassig, H. J., "Aerodynamic Flutter Coefficients for an Airfoil with Leading- and Trailing-Edge Flaps in Two-Dimensional Supersonic Flow," *Journal of Aeronautical Sciences*, Feb. 1954, pp. 131-132.

[16]Stewartson, K., "On the Linearized Potential Theory of Unsteady Supersonic Motion," *Quarterly Journal of Mechanics and Applied Mechanics*, Vol. III, Pt. 2, June 1950.

[17]Chang, C. C., "Transient Aerodynamic Behavior of an Airfoil Due to Different Arbitrary Modes of Nonstationary Motions in a Supersonic Flow," NACA TN 2333, 1951.

[18]Dengler, M. A., Goland, M., and Luke, Y. L., "Notes on the Calculation of the Response of Stable Aerodynamic Systems," *Journal of Aeronautical Sciences*, March 1952, pp. 213-214.

[19]Hassig, H. J., "An Approximate True Damping Solution of the Flutter Equations by Determinant Iteration," *Journal of Aircraft*, Nov. 1971, pp. 885-889.

[20]Jones, R. T., "The Unsteady Lift of a Wing of Finite Aspect Ratio," NACA Rept. 681, 1940.

[21]Baker, G. A. Jr., *Essentials of Padé Approximants*, Academic Press, New York, 1974.

[22]Roger, K. L., Hodges, G. E., and Felt, L., "Active Flutter Suppression—A Flight Test Demonstration," *Journal of Aircraft*, June 1975, pp. 551-556.

[23]Vepa, R., "Finite State Modeling of Aeroelastic Systems," Doctoral Disseration, Dept. of Applied Mechanics, Stanford University, Stanford, Calif., June 1975.

[24]Vepa, R., "On the Use of Padé Approximants to Represent Unsteady Aerodynamic Loads for Arbitrarily Small Motions of Wings," AIAA Paper 76-17, 1976.

[25]Theodorsen, T., "General Theory of Aerodynamic Instability and the Mechanism of Flutter," NACA Rept. No. 496, 1935.